JOURNAL OF OPTOELECTRONICS AND ADVANCED MATERIALS Vol. 9, No. 6, June 2007, p. 1825 - 1828

Influence of the recrystallization processes on the structure and magnetic properties of the $Nd_2Fe_{14}B/\alpha$-Fe nanocomposites

W. KAPPEL, M. M. CODESCU, M. VALEANU[a*], N. STANCU,
J. PINTEA, F. LIFEI[a], A. JIANU[a], D. PATROI, E. PATROI
R & D National Institute for Electrical Engineering–Advanced Research Bucharest (INCDIE ICPE-CA), Splaiul Unirii 313, sector 3, Bucharest – 030138, Romania
[a]R & D National Institute for Materials Physics Bucharest (INCDFM), Bucharest – Magurele, Romania

Exchange-coupled $Nd_2Fe_{14}B/\alpha$-Fe nanocomposite magnets receives considerable research interest, because these are regarded as promising candidate materials for permanent magnets, with an adequate performance while keeping the content of relatively expensive Nd low. The advantage of these new magnetic materials are the lower rare earth content (and consequently, cheaper magnets with better corrosion resistance). The $Nd_2Fe_{14}B/\alpha$-Fe nanocomposites were obtained by recrystallisation treatment from an amorphous phase prepared by melt-spinning. For Fe contents, between 83 and 85 at. %, we have obtained the hardening of the α-Fe phase by exchange interactions between the hard $Nd_2Fe_{14}B$ phase and the soft α-Fe phase. The evolution of the structure and main magnetic characteristics after different annealing conditions was studied. For all isotropic permanent magnets obtained from the prepared nanocomposites was measured a remanence ratio higher than 0.5, which confirm the existence of the mentioned exchange interactions.

(Received Novemebr 14, 2006; accepted April 26, 2007)

Keywords: Nanocrystalline, NdFeB, Permanent magnets

1. Introduction

First reported by the Philips group [1], the magnetic nanocomposites based on NdFeB have been studied intensively [2-4]. This new type of magnetic materials were alloys, mainly deficient in RE, composed by two nanograined phases, namely a magnetic hard phase, rich in rare earth (RE) elements, in exchange interaction with a magnetic soft phase, rich in transition metal TM, having a high saturation polarization.

The nanocomposites permanent magnets, characterized by the RE-deficiency, can become a big economic importance, because can be obtain the same performances as with sintered permanent magnets, but with lower RE contents, that means with decreased costs. It is general accepted that in order to have an exchange hardened nanocomposite with a soft and hard phase, the grain size of the soft magnetic phase must be twice the width of the Bloch wall of the hard phase [5] That means in $Nd_2Fe_{14}B/\alpha$-Fe nanocomposites a main grain size of the α-Fe phase of around 10 nm!

In nanocomposites the soft phase is α-Fe or Fe_3B and the hard phase can be $Nd_2Fe_{14}B$, $Pr_2Fe_{14}B$, $SmCo_5$, $Sm_2Fe_{17}N_x$. The enhanced remanence and the higher energy density is an advantage of nanocomposites against isotropic single-phased nanocrystalline magnets (prepared starting from microcrystalline magnetic powders), but the coercivity of the two-phase system is lower than in single-phased systems. Substitutions of Nd/Pr by Dy increase the coercivity of the system.

Schrefl [6] and Fischer [7], in their micromagnetic model of nanocomposites, explain the spring effect introduced by Kneller [2] to explain the remanence enhancement of a two-phase system: J_r, exceed the half of the saturation polarization, J_S.

2. Experimental

In the Nd-Fe-B system, our used alloys: $Nd_{11}Fe_{83}B_6$ (A1), $Nd_{10.5}Fe_{84}B_{5.5}$ (A2), $Nd_{10}Fe_{85}B_5$ (A3), are all stoechiometric, with the smallest Nd amount of only 10 at. %. The studied melt-spun samples based on NdFeB were prepared using a quartz crucible with the diameter nuzzles of 0.25 – 0.3 mm. The copper wheel velocity was v = 21-30 m/s and the overpressure of argon was 0.5 atm. The obtained NdFeB ribbons, having typically thickness in the range from 15 μm up to 50 μm, were heat treated in vacuum, at temperatures in the range 650 – 750°C, during 3 – 5 min.

3. Results and discussion

All the melt-spun alloys have amorphous structure. The XRD patterns of the $Nd_{11}Fe_{83}B_6$ (A1) before and after annealing treatment at 750°C/3 min were presented in the figure 1. We can conclude that, after melt-spinning and

annealing, the alloys shows relevant peaks, related to the Φ-phase and α-Fe. The α-Fe crystallites have sizes in the range 25 – 33 nm and crystalline ratio $R_C = A_{crist.} / A_{crist.} + A_{amorph.}$, is around 19.

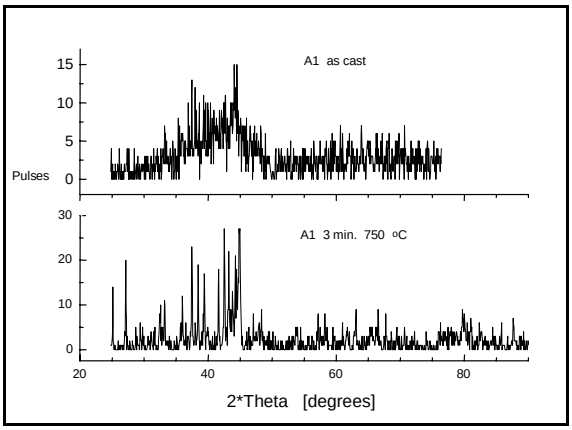

Fig.1. XRD patterns of $Nd_{11}Fe_{83}B_6$ (A1), as melt-spun and annealed at 750°C/3 min.

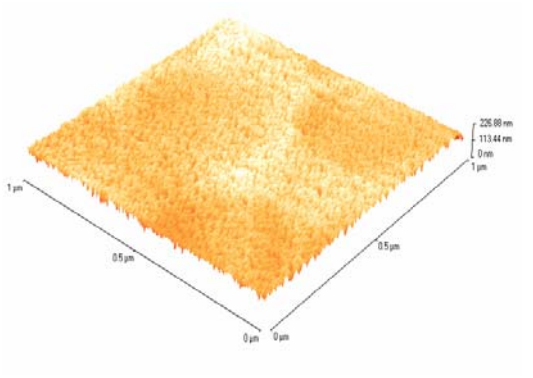

a)

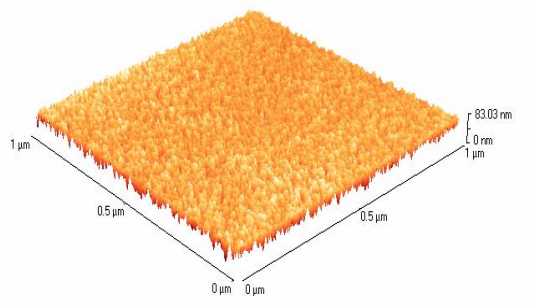

b)

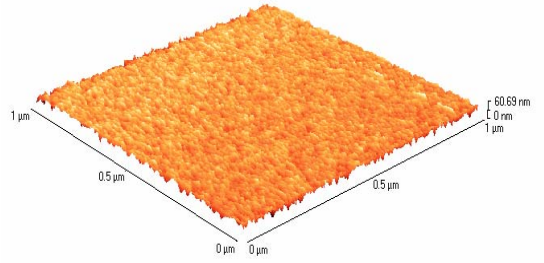

c)

Fig. 2. AFM micrographs of the $Nd_{11}Fe_{83}B_6$ a) $Nd_{10.5}Fe_{84}B_{5.5}$ b) and $Nd_{10}Fe_{85}B_5$ c) nanocrystalline ribbons.

The specific morphology of the $Nd_2Fe_{14}B/\alpha$-Fe melt-spun samples was proved by AFM investigations (see figures 2a, b and c). The structure of the ribbons is refined, with grain sizes in the nanometric range: from ~ 180 nm for $Nd_{11}Fe_{83}B_6$ grains to 55 nm $Nd_{10.5}Fe_{84}B_{5.5}$ and to 40 nm for $Nd_{10}Fe_{85}B_5$. The roughness of the surfaces decrease with the increasing of the Fe-content: from 16 nm for $Nd_{11}Fe_{83}B_6$ nanocrystalline ribbons to 9 nm for $Nd_{10.5}Fe_{84}B_{5.5}$ and to 6 nm in the case of the $Nd_{10}Fe_{85}B_5$ nanocrystalline ribbons.

The microstructure for the $Nd_{11}Fe_{83}B_6$ melt-spun alloy (A1) is shown in Fig. 3. In this micrograph emphasized a relative uniform distribution of the grain size for those two constituent phases, with grains size in the range 30…50 nm for an $Nd_2Fe_{14}B$ phase, with the clearly limits without other precipitation.

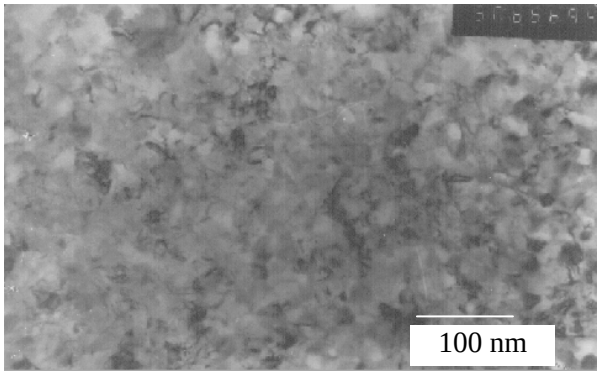

Fig. 3. TEM micrograph of a $Nd_{11}Fe_{83}B_6$ melt-spun alloy A1 ($Nd_2Fe_{14}B$ grains 30… 50 nm mean diameter, α-Fe grains ~ 20 nm means diameter).

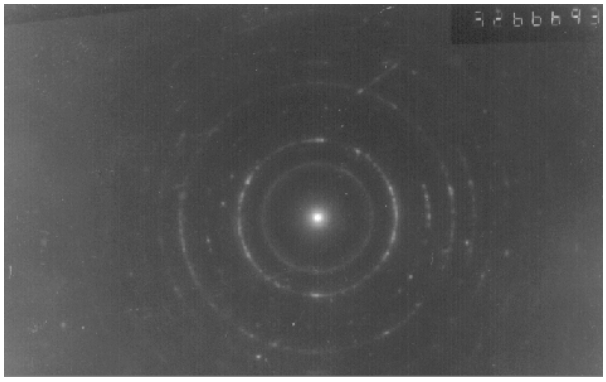

Fig. 4. The electron beam diffraction pattern of melt-spun $Nd_{11}Fe_{83}B_6$ ribbon alloy after 750°C/min. annealing Treatment.

The Fig. 4 shows the electron beam diffraction pattern for the $Nd_{11}Fe_{83}B_6$ ribbons, after 750°C/3 min. annealing treatment. For this sample, the electron beam diffraction pattern shows a high crystallization degree with nanometric dimensions.

The microstructure for the $Nd_{10}Fe_{85}B_5$ ribbon alloy, after the annealing treatment at 750 °C for 5 min., is shown in figure 5. In these micrographs it can be seen a relative

homogenous refined structure, with a grains size distribution, included in a range 20…30 nm.

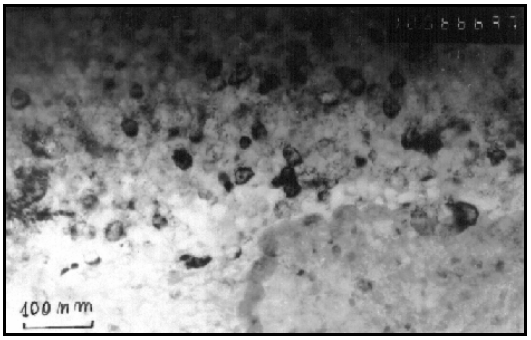

a)

b)

Fig. 5. TEM (a) and HR - TEM (b) micrograph of the $Nd_{10}Fe_{85}B_5$ ribbon (A3), after 750 °C/5 min. annealing treatment.

In Fig. 6, for the same ribbons, $Nd_{10}Fe_{85}B_5$, annealed at 750°C for 5 min., is shown the electron beam diffraction pattern, which proves, still the presence of an amorphous - state for the constituted phases. This electron beam diffraction pattern shows the degree of crystallization with the nanometric grains size.

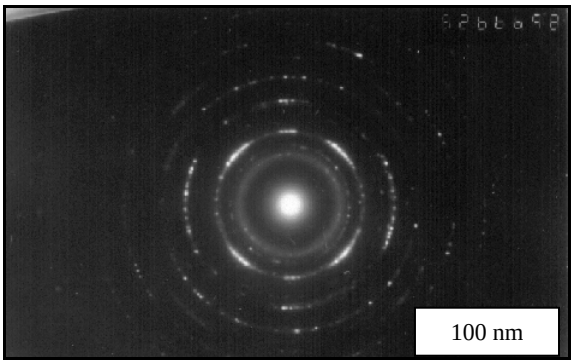

Fig. 6.The electron beam diffraction pattern of $Nd_{10}Fe_{85}B_5$ ribbons (A3), after 750 °C/5 min. annealing Treatment.

The Figs. 7 and 8 present the hysteresis curves for $Nd_{11}Fe_{83}B_6$ (A1) and $Nd_{10}Fe_{85}B_5$ (A3) alloys, for different annealing conditions. From the allure of the hysteresis curves which present a knee and related to the TEM analysis, is obvious that some samples were biphasic, their microstructure consisting in $Nd_2Fe_{14}B$ and α-Fe (see Figs. 7 and 8).

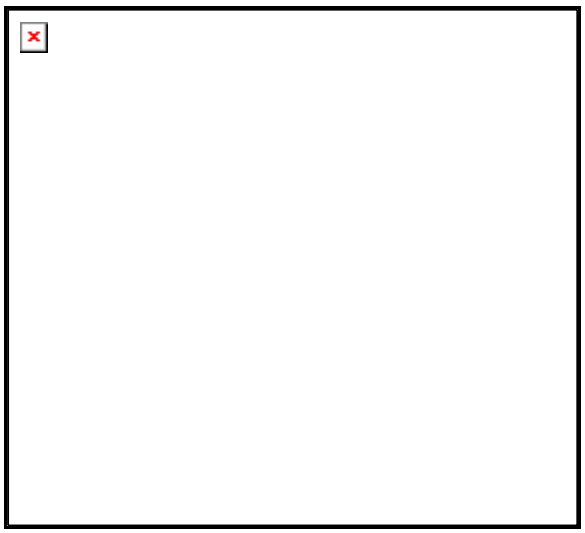

Fig. 7. Magnetic moment vs magnetic field for $Nd_{11}Fe_{83}B_6$ samples, annealed 675 °C/5 min.

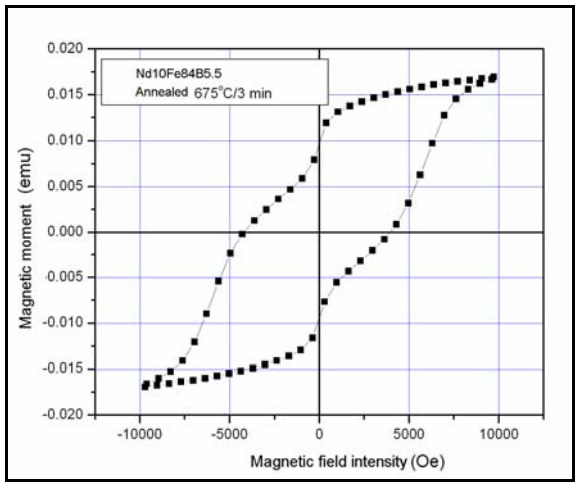

Fig. 8. Magnetic moment vs magnetic field for $Nd_{10}Fe_{85}B_5$ samples, annealed 675 °C/3 min.

Table 1 present the values of the main magnetic properties. Because the ratio of remanent magnetization and magnetization at saturation M_r/M_S is more than 0.5 [2], the obtained permanent magnets were magnetic isotropic nanocomposites, based on $Nd_2Fe_{14}B$ and α-Fe.

The values of the $_JH_c$ are top data at each Nd content which depend on preparing conditions shown in the Table 1, especially on the surface speed and annealing treatment at which α-Fe and NdFeB patterns XRD appeared, first, even in as quenched state.

Table 1. The values of the main magnetic properties: remanent magnetization M_r, magnetization at saturation M_S and coercivity $_JH_c$ for the $Nd_{11}Fe_{83}B_6$ (A1), $Nd_{10.5}Fe_{84}B_{5.5}$ (A2) and $Nd_{10}Fe_{85}B_5$ (A3) annealed alloys.

No.	Alloys (at. %)	T (^{o}C)/ t (min)	M_r (Gs)	M_S (Gs)	M_r/M_S	$_JH_c$ (kOe)
1	$Nd_{11}Fe_{83}B_6$ (A1)	650/3	159.6	282	0.566	3.2
2		675/3	532	848.6	0.627	4.0
3		700/3	284.4	501	0.567	3.3
4		725/3	311.6	496	0.628	5.1
5		750/3	129.2	231.3	0.559	4.9
7		675/5	321.7	448.4	0.720	5.6
8		700/5	347.7	499.7	0.696	5.6
9		725/5	387.6	691.6	0.560	4.0
10		750/5	169.1	291.7	0.580	5.1
13	$Nd_{105}Fe_{84}B_{5.5}$ (A2)	700/3	518.1	842.3	0.615	2.8
16		650/5	465.5	785.7	0.593	2.0
21	$Nd_{10}Fe_{85}B_5$ (A3)	650/3	310.3	600.4	0.517	2.9
22		675/3	369	642.2	0.575	4.1
25		750/3	380	549.1	0.692	2.6
26		650/5	524	800.2	0.655	2.8
27		675/5	302	427.8	0.706	4.9
28		700/5	399	631.8	0.632	3.5
29		725/5	591	815.1	0.625	4.9

The magnetic measurements show the best values magnetic characteristics for melt-spun $Nd_{11}Fe_{83}B_6$ ribbon alloy (sample A1) Nd- rich alloy, high coercivity $_JH_c \sim 5.6$ kOe and high ratio $M_r/M_S \sim 0.7$, after 675^{o}C/5 min. annealing treatments. This suggests that by the heat treatment crystal sizes become more uniformly but do not grow so bigger in our alloys.

4. Conclusions

Experimental studies of remanence enhancement and the effect of the quenching condition on rapid solidification of NdFeB melts with compositions near $Nd_2Fe_{14}B$ was investigated, by melt-spinning technique.

Nanocrystalline $Nd_2Fe_{14}B$ alloys and biphasic nanocomposites $Nd_2Fe_{14}B$ /α-Fe have been synthesized by melt-spinning and annealing treatments route, starting from $Nd_{11}Fe_{83}B_6$, Nd-rich alloys and going on with an $Nd_{10}Fe_{85}B_5$,, Nd-lower alloy.

Microstructural analyses, performed by TEM and HR-TEM, have shown for these alloys in determined conditions: wheel speed 20 - 45 m/s, annealing treatment at temperatures inn the range 650-750^{o}C for 3 - 5 min maintain times, the possibility to obtain the relative homogenous and uniform nanocrystalline structure, characterized by grains size in range 20-50 nm.

The XRD analyses show two patterns, of the soft α-Fe and hard $Nd_2Fe_{14}B$ phases. The electron beam diffraction patterns was performed and these proves the coexistence of amorphous and nanocrystalline α-Fe and $Nd_2Fe_{14}B$ phases.

No evidence has been found for the existence of significant magnetic anisotropy in such nanostructured ribbon samples.

The magnetic measurements show the best values magnetic characteristics for melt-spun $Nd_{11}Fe_{83}B_6$ ribbon alloy (sample A1) Nd- rich alloy, high coercivity $_JH_c \sim 5.6$ kOe and high ratio $M_r/M_S \sim 0.7$, after 675^{o}C/5 min. annealing treatments. This suggests that by the heat treatment the crystal size becomes more uniformly but do not grows so high than in our alloys.

Acknowledgement

The results presented in this paper were obtained in the frame of Romanian CNCSIS under the A-consortium NANOCONS grant and CEEX - Matnantech project. The dissemination of these results is supported in the frame of FP6 SSA Project No.017240/2005.

References

[1] R. Coehoorn, D. B. de Mooij, C. de Waard, J. Magn. Magn. Mat. **80**, 101(1989).
[2] E. F. Kneller, R. Hawig, IEEE Trans Magn. **27**, 3588 (1991).
[3] A. Manaf, R. A. Buckley, H. A. Davies, J. Magn. Magn. Mat. **128** (3), 302(1993).
[4] R. Skomski, J. Appl. Phys. **76**, 7059 (1994).
[5] L. H. Lewis, A. R. Moodenbaugh, D. O. Welch, V. Panchanathan, J. Phys. D.: Appl. Phys. **34**, 744 (2001).
[6] T. Schrefl, J. Fidler, D. Süss, Int. Rep. of TU Vienna, 2000.
[7] R. Fischer, T. Schrefl, H. Kronmüller, J. Fidler, J. Magn. Magn. Mat. **150**(3), 329 (1995).

*Corresponding author: valeanu@infim.ro